PNAS RESEARCH ARTICLE | IMMUNOLOGY AND INFLAMMATION

Ago2 and a miRNA reduce Topoisomerase 1 for enhancing DNA cleavage in antibody diversification by activation-induced cytidine deaminase

Maki Kobayashi[a,1], Hiroyuki Wakaguri[b], Masakazu Shimizu[b], Koichiro Higasa[b,2], Fumihiko Matsuda[b], and Tasuku Honjo[a,1]

Contributed by Tasuku Honjo; received October 8, 2022; accepted March 31, 2023; reviewed by Nayun Kim and Daisuke Kitamura

Activation-induced cytidine deaminase (AID) is the essential enzyme for imprinting immunological memory through class switch recombination (CSR) and somatic hypermutation (SHM) of the immunoglobulin (Ig) gene. AID-dependent reduction of Topoisomerase 1 (Top1) promotes DNA cleavage that occurs upon Ig gene diversification, whereas the mechanism behind AID-induced Top1 reduction remains unclear. Here, we clarified the contribution of the microRNA-Ago2 complex in AID-dependent Top1 decrease. Ago2 binds to Top1 3′UTR with two regions of AID-dependent Ago2-binding sites (5′- and 3′dABs). Top1 3′UTR knockout (3′UTRKO) in B lymphoma cells leads to decreases in DNA break efficiency in the IgH gene accompanied by a reduction in CSR and SHM frequencies. Furthermore, AID-dependent Top1 protein reduction and Ago2-binding to Top1 mRNA are down-regulated in 3′UTRKO cells. Top1 mRNA in the highly translated fractions of the sucrose gradient is decreased in an AID-dependent and Top1 3′UTR–mediated manner, resulting in a decrease in Top1 protein synthesis. Both AID and Ago2 localize in the mRNA-binding protein fractions and they interact with each other. Furthermore, we found some candidate miRNAs which possibly bind to 5′- and 3′dAB in Top1 mRNA. Among them, miR-92a-3p knockdown induces the phenotypes of 3′UTRKO cells to wild-type cells whereas it does not impact on 3′UTRKO cells. Taken together, the Ago2-miR-92a-3p complex will be recruited to Top1 3′UTR in an AID-dependent manner and posttranscriptionally reduces Top1 protein synthesis. These consequences cause the increase in a non-B-DNA structure, enhance DNA cleavage by Top1 in the Ig gene and contribute to immunological memory formation.

miRNA | RISC | genome instability | immunological memory

Significance

AID (Activation-induced cytidine deaminase) is essential for antibody diversification, such as class switch recombination (CSR) and somatic hypermutation (SHM) upon infection and immunization through immunoglobulin gene recombination. AID decreases the Topoisomerase 1 (Top1) protein to alter the DNA duplex into a non-B structure and enhance DNA cleavage; however, the underlying mechanisms of the Top1 decrease by AID are poorly understood. We found the indispensable role of Top1 3′UTR in the AID-dependent Ago2-binding for suppressing Top1 synthesis and increasing DNA cleavage. Furthermore, miR-92a-3p requires Top1 3′UTR to promote DNA cleavage and decrease Top1. Our findings suggest that this miRNA-Ago2 binds to Top1 3′UTR and reduces Top1 in an AID-dependent manner, enhancing Top1-mediated DNA cleavage, which is required for antibody diversification.

Immunoglobulin (Ig) gene diversification is necessary for developing immunological memories that enable high-affinity antibodies for the efficient eradication of micro-organisms in vertebrates. Activation-induced cytidine deaminase (AID) is the master regulator of Ig gene diversification, including class switch recombination (CSR) and somatic hypermutation (SHM) in mammals and gene conversion in birds (1–3). AID is part of the apolipoprotein B mRNA-editing enzyme catalytic polypeptide (APOBEC) RNA editing enzyme family and is composed of a cytidine deaminase domain in its center, an N-terminal domain necessary for DNA cleavage, and a C-terminal domain for DNA synapsis formation (4).

In general, Topoisomerase 1 (Top1) spreads across the nucleus, particularly accumulating in nucleoli (5). Top1 maintains the structure of the DNA duplex by removing the helical stress of DNA that is caused by transcription and replication. To resolve helical stresses, single-strand DNA is cut by forming a covalent bond between Top1's catalytic tyrosine and the 3′ phosphate end of DNA, followed by the rotation of the other free strand of DNA duplex, religation of both ends of DNA, and liberation of Top1 from the DNA duplex (6). Interestingly, Top1 inhibitors that have derived from camptothecin (CPT) and have long been used as anticancer drugs intercalate between the covalent bonds of Top1 and DNA, fix the Top1-DNA cleavage complex (Top1-cc), inhibit religation and eventually cause irreversible DNA cleavage and genomic instability (7). Similarly, Top1 can create an irreversible cleavage at damaged DNA sites, such as adducts and modifications, due to the topological difficulty which prevents the religation step (6). Therefore, Top1 is a causative enzyme for genomic instability in the DNA region of unusual properties. In fact, neuronal tissues are exposed to continuous oxidative stress and the risk of DNA damage causing Top1-cc; therefore, inhibition or mutation of Top1-cc-resolving enzymes such as ataxia telangiectasia mutated (ATM), tyrosyl-DNA phosphodiesterase 1 (TDP1), polynucleotide kinase 3′phosphatase (PNKP) and aprataxin causes prolonged Top1-cc (*SI Appendix*, Fig. S1). This unresolved Top1-cc eventually

The authors declare no competing interest.

[1]To whom correspondence may be addressed. Email: kobayashi.maki.2n@kyoto-u.ac.jp, honjo@mfour.med.kyoto-u.ac.jp.

[2]Present address: Department of Genome Analysis, Institute of Biomedical Science, Kansai Medical University, Hirakata, Osaka 573-1010, Japan.

This article contains supporting information online at https://www.pnas.org/lookup/suppl/doi:10.1073/pnas.2216918120/-/DCSupplemental.

Published April 24, 2023.

results in genomic instability, tissue damage, and developmental and neurodegenerative diseases (8–11).

On the other hand, non-B-DNA such as hairpin, cruciform, or G4 structure is known to be mutagenic and causative for gross genetic rearrangements such as translocation, deletion, and so on (12–14). However, Top1 was previously not considered a factor that impacted genomic instability in non-B-DNA regions. We had hypothesized that Top1 serves as a major player in AID-dependent DNA cleavage of V and S regions in the IgH gene during CSR and SHM (15, 16) because AID decreases Top1 protein amount to half, and furthermore, a decrease of Top1 promotes AID-dependent DNA cleavage specifically in V and S regions. Additionally, a relatively low concentration (30 nM) of Top1 inhibitor CPT could decrease CSR and SHM (15, 16). CPT anchors Top1-cc and delays its removal from DNA break ends, potentially blocking the processing mechanism toward CSR (or SHM) completion. CPT also decreased the DNA cleavage efficiency detected by terminal deoxynucleotidyl transferase (TdT) labeling method (17, 18). Supposedly Top1-cc-adducted 3′ends induced by CPT was not labeled by TdT, because TdT adds nucleotides only to simple 3′-OH DNA break ends. These results of CPT's effect indicate the specific involvement of Top1.

This hypothesis, that decreased Top1 alters B form DNA structure into non-B form and further cuts the non-B sites by Top1 itself, may even be paradoxical; however, it may be possible since AID activation reduces Top1 by half, not to zero (15). After our publication, Top1 was proved to be the causative enzyme for transcription-dependent genomic instability based on non-B-DNA-prone DNA sequences; 1) dinucleotide repeat deletion in yeast, as Top1-deleted yeast strain lacks this dinucleotide repeat instability (19, 20), 2) transcription-dependent ribonucleoside monophosphates-associated 2 to 5-bp deletion, that is Top1-dependent and generates microinstability at the misincorporated ribonucleotides in short tandem repeats analyzed in yeasts (21), 3) triplet repeat contraction, as knockdown of Top1-processing TDP1 prolongs the Top1-cc and promotes triplet repeat contraction in a transcription-coupled nucleotide excision repair–dependent manner (22). Furthermore, experimental chronic Top1 knockdown in culture cells induces accumulation of instability across the genome (23) or in exogenous triplet repeat sequences (24) in the absence of AID activation. These pieces of evidence indicate that the role of Top1 as the enzyme responsible for transcription-dependent genomic instability at non-B-DNA structure is shared in these multiple phenomena and reasonably explains Top1-dependent DNA cleavage in IgH gene diversification.

The AID-dependent Top1-mediated DNA break mechanism in the Ig gene raised three major questions: 1) how Top1 is recruited to S regions of the IgH gene and processed 2) which mechanism resolves Top1-cc at DNA cleavage sites in IgH gene, and 3) by which mechanism AID decreases Top1 protein amount. Recruitment of Top1 to AID-dependent DNA break sites requires SMARCA4, as revealed by the screening of the interacting proteins to the Top1-GFP fusion protein (25). The facilitates chromatin transcription complex is necessary for the binding of Top1 to H3K4me3, which is the marker of active transcription (25). Additionally, Top1, which covalently binds to 3′ phosphate of DNA, is degraded by ubiquitination in general (26). Therefore, Top1 binding to the S region in the IgH gene also seemed to be degraded by the proteasome, as CSR is suppressed by proteasome inhibitor Bortezomib (27). Probably this drug delays the processing of DNA break ends adducted by Top1. In contrast, the molecular mechanism underlying Top1 protein repression through AID remains unclear.

The AID-dependent decrease in Top1 was previously considered to be mediated primarily by translational repression with marginal transcriptional suppression in our publication (15). miRNA-mediated gene suppression generally causes translational suppression with or without mRNA degradation. Typically, miRNAs are converted from pri-miRNA into pre-miRNA through the microprocessor complex (DGCR8/Drosha) within the nucleus, exported to the cytoplasm, trimmed into the miRNA/miRNA duplex by DICER, loaded onto the miRNA-induced silencing complex (miRISC) consisting of Ago and trinucleotide repeat containing (TNRC) proteins and subsequently recruited to its targets (28). Argonautes, or Ago proteins, are well-known components of the RNA-induced silencing complex in small noncoding RNA-mediated posttranscriptional gene suppression, such as RNAi and miRNA (29). Four mammalian Ago proteins repress their target mRNAs (30), however, only Ago2 among these four contains a slicer activity to cleave its targets. The target RNAs are translationally suppressed in cases of mRNAs and further degraded through decapping (31). miRNA production and processing are regulated by tissue- and development-specific transcriptional programs, modification of 3′end of miRNA, or RNA-editing (28, 30), and these miRNA regulations are involved in several biological functions. In particular, conversion from adenine to inosine by adenosine deaminases (ADARs) of a subset of pri-miRNAs affects processing efficiency by Drosha or Dicer (32, 33). Although RNA editing by AID which enables AID-dependent DNA cleavage has not been delineated yet, it will be possible that AID's editing of some miRNA [or their precursor(s)] could regulate Top1 translation. Actually binding of AID to RNA is reported in polyA of mRNA (34), viral RNA (35), or germline transcripts of S regions of IgH genes (36). Furthermore, the RNA-editing activity of AID is found in viral RNA (35).

Here, we identified the molecular mechanism that underlies AID-dependent suppression of Top1 protein synthesis. Since Ago2 binds to a specific region of Top1 3′UTR in an AID-dependent manner, Top1 3′UTR knockout (3′UTRKO) cells were generated. By analyzing these cells, we clarified the requirement of Top1 3′UTR in DNA cleavage, CSR, and SHM efficiencies in conjunction with Ago2 binding to Top1 mRNA under AID activation. Furthermore, Top1 3′UTR is necessary for the AID-dependent reduction of Top1 protein synthesis. Ago2 and AID localize in RNA-binding protein fractions, and moreover, they bind to each other. A candidate miRNA, miR-92a-3p showed a positive function in AID-dependent DNA cleavage, CSR, and SHM in wild-type cells. However, this miRNA does not have an impact on these events in Top1 3′UTRKO cells, suggesting that this miRNA binds to Top1 3′UTR to achieve its function. Collectively, these pieces of evidence indicate that AID associates with the Ago2-miR-92a-3p complex and promote their binding to Top1 3′UTR for supporting the efficiency of CSR and SHM. Therefore, the miRNA-induced suppressing complex (miRISC) decreases the Top1 protein under the regulation of AID to promote DNA break efficiency.

Results

miRNA Pathway Is Involved in Efficient CSR in CH12 Cells. As miRNA pathways are well-known posttranscriptional regulators of protein synthesis, we screened proteins essential for miRNA production for their contribution to CSR induced by cytokine stimulation (CIT; IL-4, CD40 ligand and TGF-β) (*SI Appendix*, Fig. S2 *A–E*). To knockdown these factors, we used CRISPR-interference (CRISPRi, *SI Appendix*, Fig. S2*A*), the gene-specific inhibition of transcription. We generated CH12 cells stably

transfected by "dCas9-KRAB", a fusion protein of dead Cas9 enzyme and the transcriptional repressor KRAB. In these cells, the gene-specific gRNAs that target the promoter region were transiently transfected (*SI Appendix*, Fig. S2*A*) (37). Knockdown of Drosha, DGCR8, and Ago2 significantly decreased CSR efficiency to less than half of the control (*SI Appendix*, Fig. S2*B*) when their expression is suppressed less than 20% of the control (*SI Appendix*, Fig. S2*C*). In contrast, knockdown of Dicer does not alter CSR efficiency, indicating that this miRNA pathway functioning in AID-dependent CSR may be noncanonical, Dicer-independent and may instead be processed by Ago2 (38, 39). AID transcripts are modestly (~60%) decreased by knockdown of Ago1 and Ago2, whereas this level of effect does not explain the CSR decrease (*SI Appendix*, Fig. S2*D*). Knockdown of these molecules does not affect the expression of the Sμ- and Sα-germline transcripts (*SI Appendix*, Fig. S2*E*), suggesting the contribution of miRNA pathways in CSR.

Ago2 Binds to the Specific Sites of Top1 mRNA in an AID-Dependent Manner. The miRNA pathway's involvement in the regulation of CSR efficiency is shown; therefore, we examined the binding between Ago2 and Top1 mRNA. Using immunoprecipitation of formaldehyde-fixed cell lysates (FA-RNA-IP) with an anti-Ago2 antibody (Fig. 1 *A* and *B*), the AID-dependent Ago2 binding to Top1 mRNA was revealed by the three different primer sets (cA, 3uB, and 3uC).

Since mapping of Ago2-binding sites with single-nucleotide resolution suggests the putative binding miRNAs, specific binding sites of Ago2 to Top1 mRNA were identified using photoactivatable ribonucleoside cross-linking and immunoprecipitation (PAR-CLIP) methods (Fig. 1 *C*–*G*, *SI Appendix*, Fig. S3, and Datasets S1–S4) (40). In this experiment, we utilized an inducible AID molecule, AID-ER (41) to introduce AID in 293T cells that do not express endogenous AID. AID-ER is a fusion protein of AID and the ligand-binding domain of an estrogen receptor mutant, ER-T2 and it is activated by a conformational change upon binding of the estrogen analog, 4-hydroxytamoxifen (4-OHT) (42, 43).

As depicted in Fig. 1*C*, HEK293T cells that expressed AID-ER (293T AID-ER) or the dead mutant AID, KSS-ER (293T KSS-ER) (15) were incubated with 4-thiouridine (4-SU), irradiated by 365-nm UV and their lysates were immunoprecipitated by the anti-Ago2 antibody. Because the 4-SU, which is incorporated in Top1 mRNA and cross-linked with the sulfate group in Ago2 by UV, forms a base-pair with guanine (G) instead of adenine during reverse transcription, uridine (U) to cytosine (C) conversion in sequencing results indicates a footprint of Ago2-binding. When the Top1 mRNA is bound by the other protein, U to C conversion by this binding will occur during PAR-CLIP procedure; however, such Top1 mRNAs will not be enriched by anti-Ago2 antibody.

In recovered cDNA fractions, the coding region (251st-2,548th of Top1 mRNA) and the 3′UTR (2,549th-3,629th) of Top1 mRNA (total 3,738 nt) were amplified using PCR and analyzed with next-generation sequencing (Fig. 1 *D* and *E*). Top1 mRNA from 293T-AID-ER cells shows the remarkable peaks of AID-specific U to C conversion at the proximal region of 3′UTR (5′- and 3′dABs, Fig. 1*E*). These peaks do not appear in 293T-KSS-ER. The frequency of the 5′ peak in the AID-dependent U to C is 10.9% at 2,654th and that of the 3′ peak is 25.1% at 2,672nd. This outcome is reproduced in the other dataset (*SI Appendix*, Fig. S3), as the 5′ peak of the Ago2-dependent U to C is 14.8% at 2,657th and the 3′ two peaks are 22.8% at 2,670th and 22.2% at 2,673rd. We named the 2,654th and 2,657th Us as 5′ AID-dependent Ago2-binding sites (5′dABs) and the 2,670th, 2,672nd, and 2,673rd Us as 3′ dAB sites. Comparably, the peaks of U to C conversion from 3,004th to 3,006th are detected in both AID-ER and KSS-ER cells; therefore we named them AID-independent Ago2-binding sites (iABs).

To confirm whether these 5′- and 3′dABs and iABs are Ago2-dependent or not, the corresponding Top1 3′UTR regions were sequenced by Sanger sequencing, using the RNA fractions from the 293T-AID-ER and 293T-KSS-ER cells similarly prepared using 4-SU and 365-nm UV-irradiation, but not immunoprecipitated with anti-Ago2 antibody. As a result, these AID-dependent and independent U to C peaks were not observed in the samples without IP (Fig. 1 *F* and *G* and Dataset S3), indicating that these dABs and iABs are dependent on Ago2.

Deletion of Top1 3′UTR in CH12 Cells Decreases AID-Dependent CSR and SHM by Downregulation of DNA Break Frequencies. To identify the function of Top1 3′UTR in AID-induced CSR, this 3′UTR was knocked out in CH12 F3-2A cells by CRISPR/Cas9 technology (*SI Appendix*, Fig. S4). To observe the effect of 3′UTR knockout without the influence of endogenous AID, exogenous and inducible AID-ER was introduced.

Initially the 3′UTRKO-A and -C cells were evaluated for their CSR, SHM in the 5′ Sμ region, germline transcripts, and Top1 mRNA (*SI Appendix*, Fig. S5 *A*–*E* and Table S1). The 3′UTRKO-A and -C cells showed lower CSR (*SI Appendix*, Fig. S5*A*) and SHM efficiency (*SI Appendix*, Fig. S5 *B* and *C* and Table S1) without a decrease in germline transcripts of Sμ- and Sα- switch regions (*SI Appendix*, Fig. S5*D*). Top1 mRNA with or without AID activation increased in 3′UTRKO cells (*SI Appendix*, Fig. S5*E*).

However, endogenous AID in 3′UTRKO-C cells was lower than in other cells (*SI Appendix*, Fig. S5 *F* and *G*); therefore, monoclonal cells among these 3′UTRKO cells were established through limited dilution to pick up the cell lines that express AID and AID-ER-3XFLAG equally (Fig. 2 *A* and *B*). Since wild-type #215 (W215), 3′UTR KO-A #102 (A102), B#43 (B43), C#1 (C1) showed similar AID and AID-ER expression, these clones were used for further analysis. The germline transcripts analyzed with the several primer sets, which cover I promoters and S regions, did not show any decrease in 3′UTR-KO cell transcripts compared to wild-type cells (*SI Appendix*, Fig. S6).

The CSR efficiency of all 3′UTRKO cloned cells, A102, B43, and C1, were significantly lower than that of wild-type cells (Fig. 2*C*). SHM of the 399 bp region 5′ to the repetitive core Sμ region was analyzed (*SI Appendix*, Fig. S5*B*). SHM frequencies of these 3′UTRKO clones were also significantly lower compared to the wild-type (Fig. 2*D* and *SI Appendix*, Table S2). To test whether these lower CSR and SHM frequencies were caused by DNA break insufficiency, AID-dependent DNA break level was analyzed using DNA break assay with biotin-dUTP (Bio-dUTP) labeling (Fig. 2 *E* and *F* and *SI Appendix*, Fig. S7).

Since 3′ DNA ends cleaved by Top1 is likely to retain 3′-phosphate (*SI Appendix*, Fig. S1) (6, 44), our previous method was modified to include the step removing 3′phosphate by T4 polynucleotide kinase (PNK) with 3′phosphatase activity (3′PTP) prior to the labeling (Fig. 2*E*) (18). The treated 3′OH-DNA break ends were then labeled by Bio-dUTP and TdT. The result showed a reduction in DNA break frequency in the 3'UTRKO cells compared to the wild-type cells (Fig. 2*F* and *SI Appendix*, Fig. S7), demonstrating that their lower CSR and SHM than wild-type cells are due to the suppression of the DNA cleavage step but not the repair step. When DNA was processed by T4PNK without 3′PTP activity, the DNA break signal in W215 cells was lower than that with 3′PTP, indicating the presence of 3′phosphate and suggesting the contribution of Top1 in AID-dependent DNA cleavage (*SI Appendix*, Fig. S1).

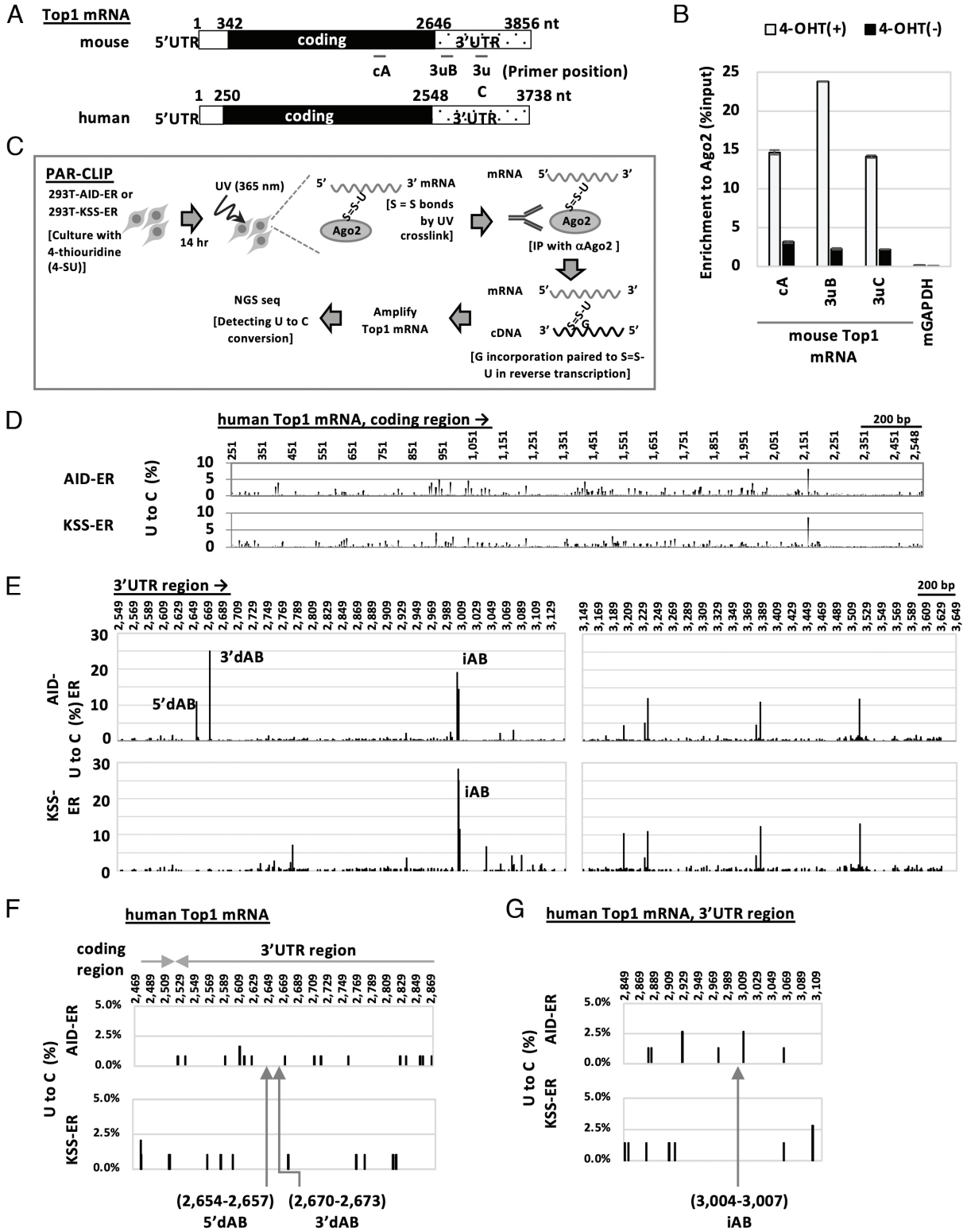

Fig. 1. Ago2 directly binds to the specific region of 3′UTR of Top1 mRNA. (*A*) (*Top*) The position of the primer sets in mouse Top1 mRNA. Primer sequences are described in Dataset S5. (*Bottom*) Structure of human Top1 mRNA in HEK293T cells. (*B*) Top1 mRNA recruitment to Ago2 analyzed by RNA immunoprecipitation with formaldehyde-crosslinking (FA-RNA-IP) and anti-Ago2 antibody in CH12 cells expressing AID-ER. Enrichment to Ago2 was shown by %input, the mean ± SD of a qPCR experiment. (*C*) Scheme of the photoactivatable ribonucleoside cross-linking and immunoprecipitation (PAR-CLIP) used for identification of Ago2-binding sites in Top1 mRNA. (*D* and *E*) Locus-specific Ago2-binding sites detected by the PAR-CLIP assay and next-generation sequencing, focusing on the Top1 coding region (*D*) and Top1 3′UTR region (*E*). The Top1 3′UTR has two AID-dependent Ago2-binding sites (5′- and 3′ dABs) and an AID-independent Ago2-binding site (iABs). The repetitive analysis yielded a reproducible result (*SI Appendix*, Fig. S3). (*F* and *G*) Sanger sequencing of the partial Top1 mRNA regions corresponding to 5′-, 3′dABs (*F*) and iAB (*G*) using total RNA from 293T-AID-ER and 293T-KSS-ER. These cells were treated by 4-SU and irradiated by 365 nm UV, but not processed by RNA-IP with anti-Ago2 antibody.

Top1 3′UTR Is Necessary for Both of Ago2 Binding to Top1 mRNA and AID-Dependent Top1 Protein Depletion. As Ago2 binds to Top1 3′UTR (Fig. 1), a requirement of 3′UTR in Ago2 binding to Top1 mRNA was analyzed in wild-type and 3′UTRKO-C1 cells with FA-RNA-IP using an anti-Ago2 antibody (Fig. 3 *A* and *B*). In wild-type cells, AID-activated samples showed greater enrichment

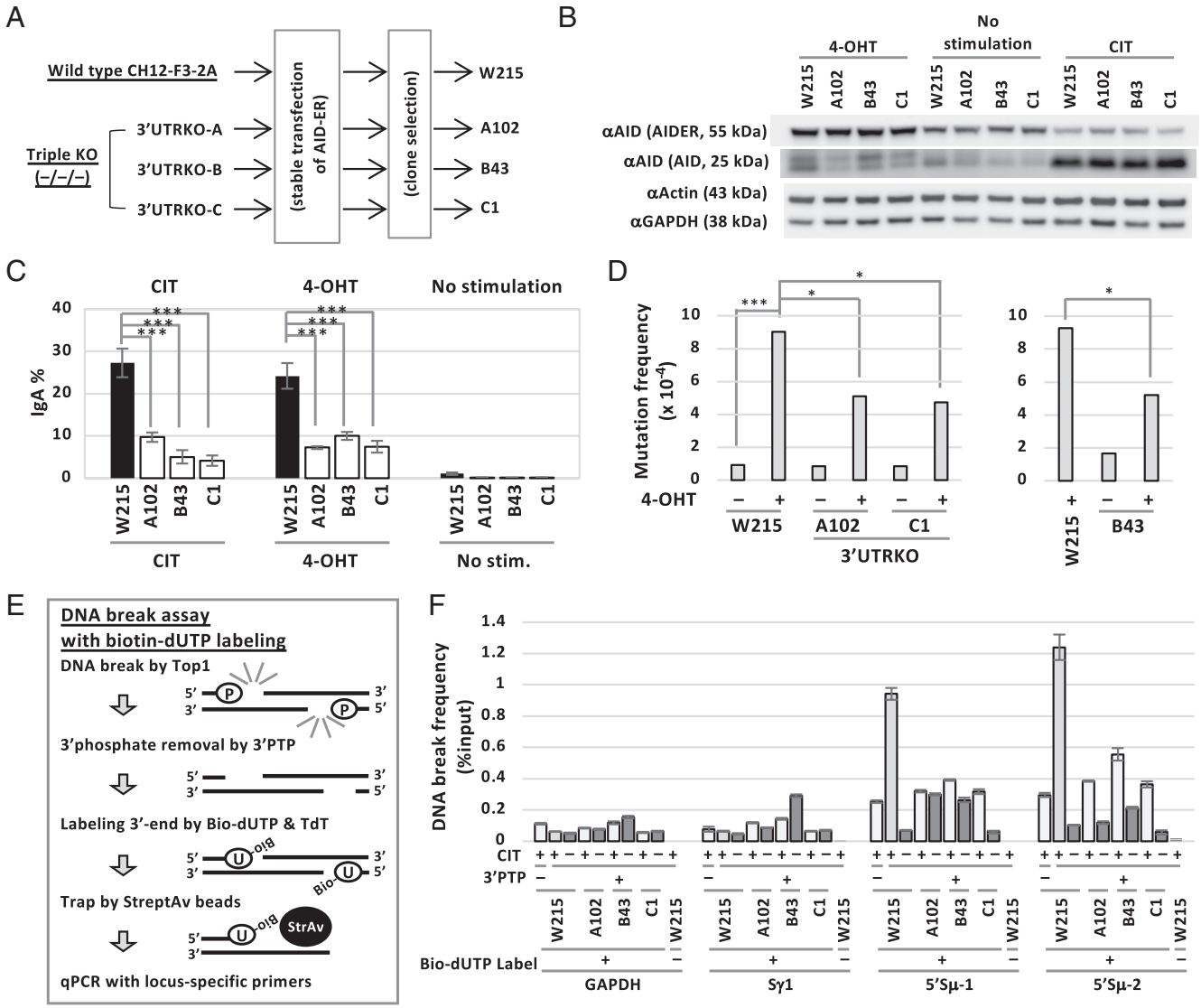

Fig. 2. Deletion of Top1 3′UTR in CH12 cells decreases AID-dependent CSR and SHM by downregulation of DNA break frequencies. (*A*) Isolation of monoclonal cells from wild-type and Top1 3′UTRKO CH12 cells after stable AID-ER introduction. From wild-type cells, W215 cells were isolated. A102, B43, and C1 cells were isolated from the three independent clones of Top1 3′UTRKO cell lines, 3′UTRKO-A, -B and -C, respectively. (*B*) AID and AID-ER amounts in wild-type and 3′UTRKO cell lines shown by western blot. Representative pictures of the three independent experiments are shown. (*C*) CSR to IgA in the wild-type and 3′UTRKO cell lines. The mean ± SD of three experiments of IgA% is shown. Statistical significance was calculated using Student's *t* test. ***$P < 0.001$. (*D*) Somatic hypermutation frequency in wild-type cells and 3′UTRKO cells. Statistical significance was calculated using Fisher's exact test. (*Left*) W215, A102, and C1 cells were compared. (*Right*) W215 and B43 cells were compared. *$P < 0.05$; ***$P < 0.001$. (*E*) Illustration of DNA break assay with biotin-dUTP labeling. 3′PTP + or –, T4 polynucleotide kinase with or without 3′ phosphatase activity; Bio-dUTP, biotinylated 16-dUTP; TdT, terminal deoxynucleotidyl transferase; StreptAv, streptavidin beads. (*F*) DNA break frequency detected by biotin-dUTP labeling in the wild-type and Top1 3′UTRKO CH12 cells, stimulated or non-stimulated with CIT. DNA break level in the Sμ region and the control GAPDH and Sγ1 regions was evaluated. The primer sequences are shown in Dataset S5.

than nonactivated cells in all coding primer sets and 3′UTR regions as expected. Compared to that, the enrichment signal of the Top1 coding region in Top1 3′UTKO C1 cells decreased to less than half of that in the wild-type cells, as demonstrated by the three different primer sets. These results indicate that Top1 3′UTR is required for AID-dependent Top1 protein reduction because Ago2-binding to Top1 mRNA largely depends on 3′UTR.

Since binding of the complex of Ago2 and miRNA to 3′UTR generally results in the elimination of mRNA and translational suppression, we evaluated the effect of 3′UTR deletion on AID-dependent Top1 reduction by detecting soluble Top1 protein to PBS-TritonX100 buffer in W215 and 3′UTRKO-A102, -B43 and -C1 cells as well as AID knockout (AIDKO) cells (Fig. 3*C*). Measurement of the soluble Top1 protein amount using ImageJ and normalized to actin revealed that soluble Top1 was decreased by AID activation only in wild-type cells while it was retained in Top1 3′UTRKO cells even after AID activation (Top1/Actin). AIDKO cells also showed no decrease in soluble Top1 protein. The difference in AID-dependent Top1 reduction between wild-type and 3′UTRKO cells suggests that 3′UTR is the sensor of the AID's function and essential for this Top1 reduction.

To check for the correlation between Top1 protein and its mRNA, total Top1 mRNA in whole-cell extracts was examined (*SI Appendix*, Fig. S8). The results show that 4-OHT stimulation does not change the total Top1 mRNA level but CIT stimulation reduces Top1 mRNA. However, CI and CIT stimulations also decrease total Top1 mRNA even in the absence of AID as AIDKO cells show, suggesting that this change is not dependent on AID's function but on cytokine stimulation. Comparing the soluble Top1 protein and total Top1 mRNA, soluble Top1 protein change was not explained by total Top1 mRNA recovered from whole cells.

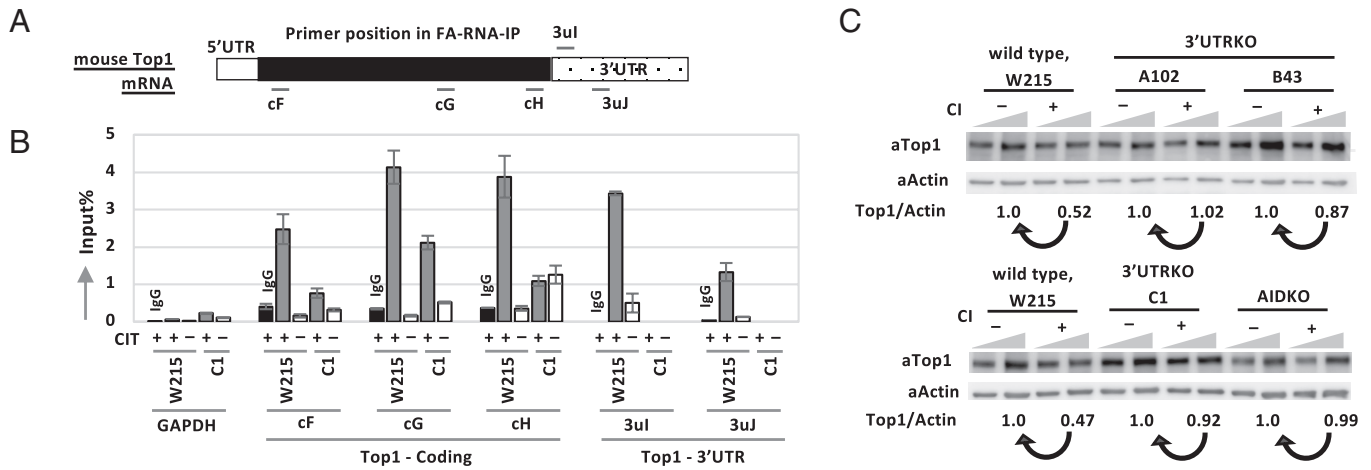

Fig. 3. Top1 3′UTR is necessary for AID-dependent Top1 protein depletion as well as Ago2 binding to Top1 mRNA. (*A*) Mouse Top1 mRNA and primer sets used for qRT-PCR in the Ago2-FA-RNA-IP experiment (*B*). (*B*) Enrichment of Top1 and GAPDH mRNA to Ago2 protein analyzed by FA-RNA-IP with an anti-Ago2 antibody. The mean ± SD of the triplicate wells of the qPCR analysis is shown. The primer sequences are shown in Dataset S5. (*C*) Western blot of wild-type and 3′UTRKO cells, showing Top1 protein amounts in PBS-TritonX-100 fraction after AID activation. The representative picture of the three experiments is shown. AIDKO cells do not harbor AID-ER. The triangles show the loading amount of the lysates, the right lane contains 1.5 volume of the left lane in each sample. The Top1/Actin ratio was compared between the stimulated and the non-stimulated cells of each cell line. Arrows indicate the two samples compared.

Top1 3′UTR Is Necessary for AID-Dependent Repression of Top1 Protein Synthesis. Because the analysis of total Top1 mRNA does not correlate with the soluble Top1 protein, AID-dependent change of Top1 translation was examined by polysome fractionation (Fig. 4*A*) (45) in wild-type and 3′UTRKO-C1 cells three times. The experiments were named Exp1 (AID-ER activation by 4-OHT, Fig. 4 *B*–*I*), Exp2 (AID-ER activation, *SI Appendix*, Fig. S9), and Exp3 (endogenous AID activation by CIT, *SI Appendix*, Fig. S10). The plots of optical density (OD) at 254 nm showed no difference in the global translation profile between wild-type and Top1 3′UTRKO cells (Fig. 4*B* and *SI Appendix*, Figs. S9*A* and S10 *A* and *B*).

Distribution of Top1 and other mRNAs was examined in the pooled ten fractions (#1-#10) as well as upper (up), and bottom (bottom) sucrose solutions (Fig. 4*A*). The input amount of Top1 mRNA was higher in 3′UTRKO-C1 cells than W215 cells, though, each mRNA showed an almost equal level of the input amount among the four samples, W215 and 3′UTRKO-C1 cells with or without stimulation in Exp1 and Exp2 (Fig. 4*D* and *SI Appendix*, Fig. S9*B*). We calculated the recovery ratio of each mRNA in the fractions by comparing the mRNA amount of each fraction and input (%input). Recovery ratio of Top1 mRNA showed a decrease especially in the highly translated, the pooled RNA fractions #8, in AID-activated cells compared to the nonstimulated wild-type cells, whereas this decrease via AID activation was not observed in the 3′UTRKO-C1 cells (Fig. 4*E* and *SI Appendix*, Fig. S9*C* and S10 *D* and *E*). This means that the AID-dependent decrease in the recovered Top1 mRNA in the highly translated fractions required the 3′UTR. Additionally, Top1 mRNA was widely distributed in the lighter fractions in 3′UTRKO-C1 cells, whereas it was mostly localized to fraction #8 at ~40% input in W215 cells. This indicates that not all of the increased Top1 mRNAs in 3′UTRKO cells was translated. The control beta-2 microglobulin (β2M) mRNA distribution did not show the difference between wild-type and 3′UTRKO cells and was not affected by the presence or absence of AID activation (Fig. 4*F* and *SI Appendix*, Figs. S9*D* and S10 *F* and *G*).

Top1 and β2M mRNAs are 3,856 and 860 nucleotides (nt) in mice, respectively; therefore, the distribution of longer mRNA is supposed to shift toward the heavy side, the highly translated polysome fractions. Topoisomerase 2 alpha (Top2a) of 5,221 nt and topoisomerase three alpha (Top3a) of 3,741-nt mRNAs were examined to check the quality of the heavy fractions around #8. As shown in Fig. 4 *G* and *H* and *SI Appendix*, Fig. S9 *E* and *F*, distribution peaks of Top2a and Top3a mRNAs in the fractions #9 and #6-#7 certified the quality of the heavy fractions obtained from the stimulated W215 cells. Their distribution patterns also did not reveal any difference between the analyzed four samples, suggesting the specificity of AID-dependent and 3′UTR-mediated Top1 mRNA decrease in the heavy fractions.

The total recovery rate, or the summation of the recovery rate of each fraction, was calculated in Exp1–Exp3 (Fig. 4*I*). Surprisingly, the total recovery rate (%input) did not reach 100% in all the mRNAs examined here, showing that some sort of loss of mRNA generally occurs during polysome fractionation. Notably, Top2a was recovered only at ~40% of input. However, it is unlikely that this loss of mRNA is due to a simple, random, and artificial degradation by technical problems, because 1) β2M, Top2a and Top3a mRNAs were recovered at a similar level from the four samples examined here, and 2) their total recovery rate is reproducible throughout the Exp1–Exp3, suggesting some underlying mechanism proprietary to each mRNA. Particularly, more decrease in Top1 mRNA recovery rate in AID-activated cells was only observed in wild-type cells but not in 3′UTRKO cells. Together, translational block was not detected unexpectedly, but the specific decrease in Top1 mRNA in an AID- and Top1 3′UTR-dependent manner was observed.

To examine the Top1 protein synthesis directly, the newly synthesized Top1 protein was examined by the azidohomoalanine (AHA) method (Fig. 4 *J*–*L*) as previously performed (15). After incubation of AID-ER-activated cells with AHA in culture, their lysates were biotinylated and the purified proteins from them were trapped by streptavidin beads (Fig. 4*J*). The newly synthesized Top1 amount averaged from the three independent experiments revealed that the newly synthesized Top1 was reduced by 0.2 μM 4-OHT-stimulation only in W215 cells, whereas that in Top1 3′UTRKO-C1 cells was not decreased by AID-ER activation (Fig. 4 *K* and *L*). This result supports the finding that the AID-dependent decrease in Top1 protein synthesis requires Top1 3′UTR.

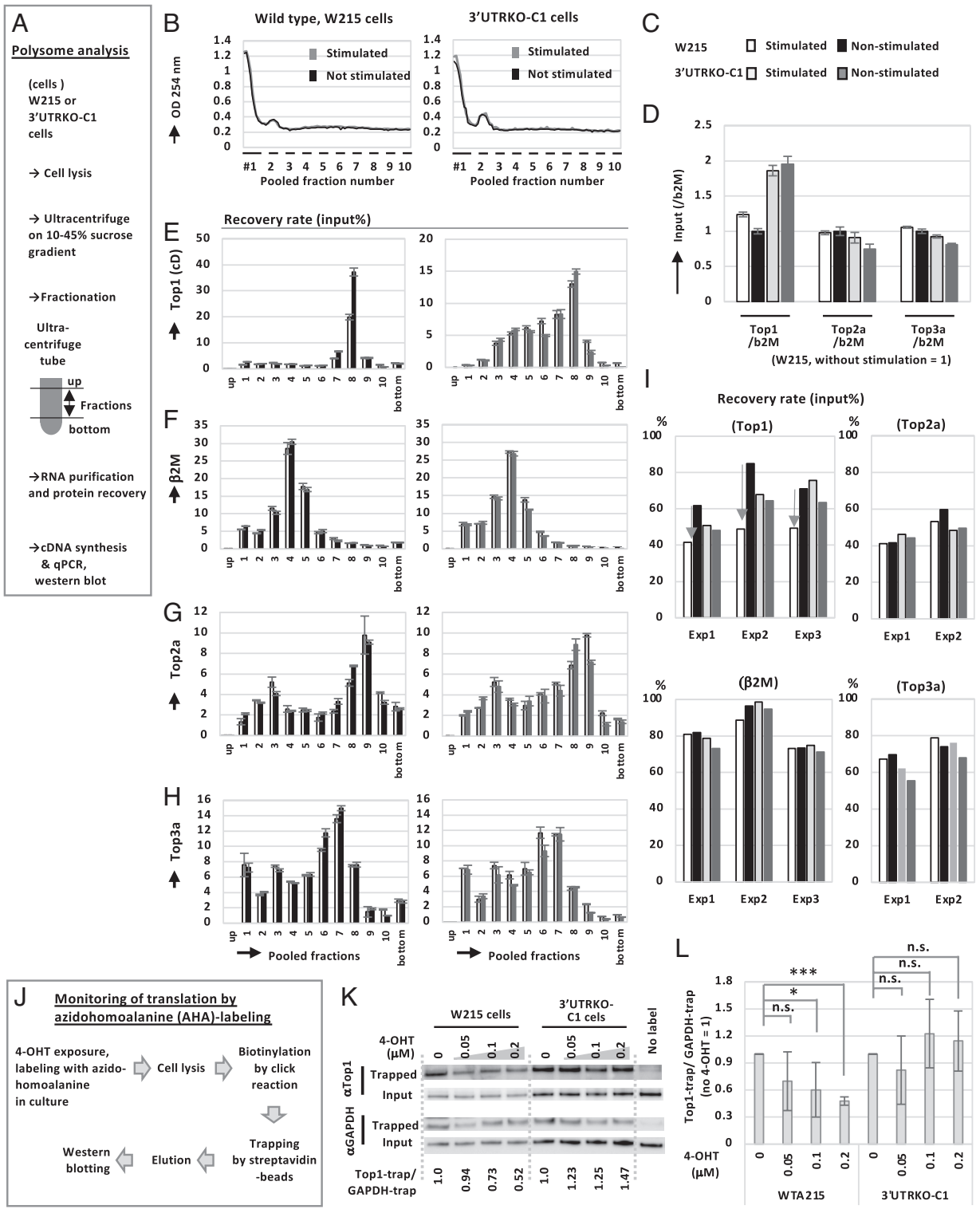

Fig. 4. AID-dependent suppression of Top1 protein synthesis is mediated byTop1 3′UTR. (*A*) Illustration of polysome analysis procedure for evaluation of translation of Top1 mRNA. (*B–I*) The results of Exp1 among the polysome fractionation experiments performed three times. The results of Exp2 and Exp3 are shown in *SI Appendix*, Figs. S9 and S10. (*B*) Optical density at 254 nm of each fraction of polysome analysis from wild-type W215 (*Left*) and 3′UTRKO-C1 (*Right*) cells. (*C*) Color codes for W215 and 3′UTRKO-C1, which are stimulated and nonstimulated. The codes are shared throughout Fig. 4 (*D–I*) and *SI Appendix*, Figs. S9 *B–F* and S10 *C–G*. (*D*) Input mRNA amount of Top1, DNA topoisomerase 2 alpha (Top2a) and DNA topoisomerase three alpha (Top3a) normalized by β2M. The signals are normalized by the signal of the nonstimulated (NS) W215 cells' value (=1). (*E–H*) mRNA distribution in the polysome fractions analyzed by RT-qPCR. Top1 (*E*), β2M (*F*), Top2a (*G*), and (Top3a) (*H*) mRNA from 4-OHT-stimulated or not stimulated W215 and 3′UTRKO-C1 cells. The mean ± SD of the triplicate wells of the qPCR analysis is shown. Primer sequences are displayed in Dataset S5. (*I*) Total recovery rate of each mRNAs analyzed in the polysome fractionation, shown as % to each input amount (%input). Exp1 are the data from Fig. 4 (*E–H*), Exp2 from *SI Appendix*, Fig. S9 *C–F* and Exp3 from *SI Appendix*, Fig. S10 *D–G*. Arrows indicate decrease in total recovery rate in Top1 mRNA. (*J*) Illustration of the method for monitoring of the newly translated proteins by L-azidohomoalanine (AHA)-labeling. Newly synthesized Top1 and GAPDH were detected. (*K*) Representative western blot picture of newly synthesized Top1 and GAPDH in W215 and 3′UTRKO-C1 cells stimulated by the indicated concentration of 4-OHT. "Trapped" shows the newly synthesized proteins. The triangles mean the increment of 4-OHT concentration used in each lane. (*L*) The band intensity of Top1 and GAPDH of western blot pictures of three independent experiments was measured by ImageJ and tested by Student's *t* test.

AID Localizes to RNA-Binding Protein Fractions and Binds to Ago2. Because the binding of Ago2 to Top1 3′UTR was observed (Fig. 1), the distribution of Ago2 in polysome fractions was examined (Fig. 5*A* and *SI Appendix*, Fig. S11). As previously reported, Ago2 localizes polysome fractions widely because of its RNA-binding ability (46). To estimate AID's function in the regulation of Top1 mRNA, the distribution of AID-ER or AID was also tested. Interestingly, 4-OHT-activated AID-ER localizes in the wide range of polysome fractions similar to Ago2, while nonactivated AID-ER localizes limitedly in the upper and #1-#2 fractions. It suggests that AID-ER acquires RNA-binding capacity only upon 4-OHT activation. These distributions of Ago2 and AID-ER were observed even in 3′UTRKO-C1 cells, indicating their RNA-binding capacity to the other RNA than Top1 mRNA. Ribosomal protein large 26 (RPL26) is a representative ribosomal protein localizing in polysome fractions (47). βActin (Act-b) and GAPDH remain in the upper and #1 fractions because they are cytoskeleton and cytoplasmic enzyme proteins, respectively.

As Ago2 and AID localize to a similar range of RNA-binding protein fractions, the interaction between Ago2 and AID was tested by coimmunoprecipitation (Fig. 5 *B* and *C* and *SI Appendix*, Fig. S12). The 3XFLAG-tagged AID-ER traps Ago2 (Fig. 5*B* and *SI Appendix*, Fig. S12 *A* and *B*) and inversely, 3XFLAG-tagged Ago2 pull down the endogenous AID (Fig. 5*C* and *SI Appendix*, Fig. S12*C*). This suggests that AID may possibly bind to Ago2 for the regulation of miRNA-mediated binding to Top1 mRNA.

Selection of the Candidate miRNAs Binding to 5′- or 3′ dAB Sites of Top1 3′UTR from Ago2-Binding miRNA Fractions. The AID-dependent Ago2-binding sites in Top1 mRNA (Fig. 1) suggested that Top1 mRNA is regulated by miR-Ago2 complex, especially upon activation of AID. To identify potential miRNAs that bind to Top1 3′UTR, the libraries of small RNA fractions of 293T-AID-ER and 293T-KSS-ER enriched to Ago2 were prepared using PAR-CLIP methods, then sequenced using SOLiD deep sequencing (Dataset S4). The obtained reads were filtered according to the following (*SI Appendix*, Fig. S13 *A–C* and Dataset S4): their read numbers, the ratio of expression frequencies in AID-ER cells vs. that in KSS-ER cells, their conservations between humans, mice, and rats, and the possible alignment with flanking sequences of 5′- and 3′dAB sites. Since not only the seed region but also its 3′ side sequences contribute to miRNA binding with targets (48, 49), the alignment of the conserved 21 putative miRNAs to the 5′- and 3′dAB in Top1 mRNA were manually assessed (*SI Appendix*, Fig. S13*C* and Dataset S4). miRNA binding to the region of Top1 3′UTR was deemed possible if the serial matching nucleotide number extends beyond six. As a result, 10 sequences of miRNA candidates, converged into the six putative miRNAs, remained as the candidates binding to Top1 3′UTR (*SI Appendix*, Fig. S13 *B* and *C* and Dataset S4). These were divided into two groups; 5 miRNAs related to 5′dAB and a miRNA related to 3′dAB. Although miR-499 was not included among these six candidates, the TargetScanMouse 7.2, a prediction tool of miRNA to 3′UTR of mRNAs suggested this miRNA's binding to 5′dAB in Top1 3′UTR.

We examined the enrollment of these candidate miRNAs, miR-92a-3p, miR-320a-3p, miR-378-3p, miR-532-5p, miR-125b-1, and miR-193a-5p in CSR through overexpression by miRNA mimics or inhibition by locked nucleic acid (LNA) oligos. As observed in our findings (*SI Appendix*, Fig. S13*D*), the overexpression of miR-92a-3p slightly up-regulates, and its inhibition down-regulates CSR, showing that the amount of miR-92a-3p tended to correlate

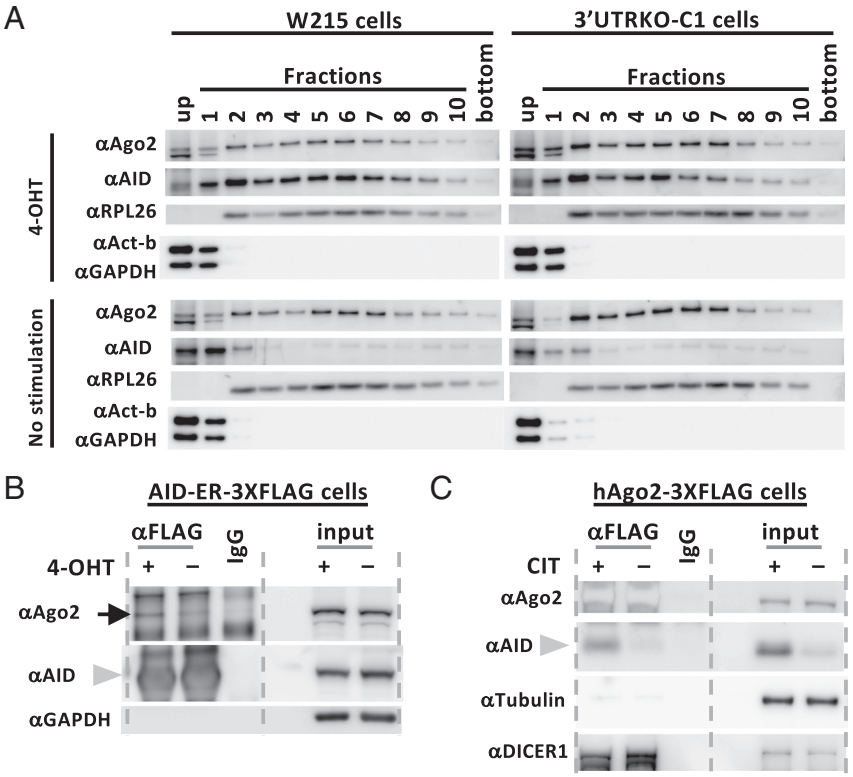

Fig. 5. Ago2 and AID localize in RNA-binding fractions and AID interacts with Ago2. (*A*) Distribution of Ago2 and AID in the polysome fraction samples shown in Fig. 4 (*B–I*). Anti-ribosomal protein large 26 (RPL26) antibody was used as the control, showing the protein recovery from each fraction. Anti-β-actin(Act-b) and -GAPDH antibodies were used as the control of the proteins that do not bind to RNA. (*B* and *C*) Interaction of AID and Ago2 proteins detected by coimmunoprecipitation. The cells that overexpressed either 3XFLAG-tagged AID-ER (*B*) or 3XFLAG-tagged human Ago2 (hAgo2) (*C*) were used. An arrow and arrowheads show ago2 and AID-ER (*B*) or AID (*C*), respectively. The reproducible data are shown in *SI Appendix*, Fig. S12.

with AID-dependent CSR. It is unclear why the inhibitory efficiency of miR-92a-3p is higher than its overexpression efficiency; however, one possible reason could be the abundance of miR-92a-3p, which is highly expressed in B lymphocytes compared to the other candidate miRNAs, as shown in *SI Appendix*, Fig. S13*B* and Dataset S4. Therefore, inhibiting miR-92a-3p may be easier than overexpressing it. The other five miRNA mimics marginally affect CSR efficiency.

The effect of these candidate miRNAs on Top1 protein amount was tested (*SI Appendix*, Fig. S14). Since the change in IgA expression was modest upon overexpression of these miRNAs, a small difference in Top1 protein levels was expected. As a result, all 4-OHT-stimulated cells with miRNA overexpression showed a decrease in Top1 protein levels to almost half that of the control (*SI Appendix*, Fig. S14*A*). Additionally, even the 4-OHT-stimulated cells with miR-92a-3p overexpression, which showed slight upregulation of IgA expression, did not exhibit further decreases in Top1 protein levels. Supporting this, there was a correlation between the abundance of Top1 protein and the intensity measured in the western blot picture; however, the sensitivity of this method was not high enough to detect small differences in Top1 protein levels (*SI Appendix*, Fig. S14*B*). Therefore, the difference in Top1 protein decrease upon AID activation between the cells with control and miR-92a-3p overexpression was not detected. In contrast, the effect of inhibiting miR-92a-3p on Top1 protein levels was clear, as the decrease in Top1 protein caused by AID activation was abolished in miR-92a-3p inhibition cells (*SI Appendix*, Fig. S14*C*), likely due to a sufficient difference in IgA expression (~30% of the control) in this case.

miR-92a-3p Contributes to AID-Dependent DNA Cleavage and Top1 Protein Reduction through 3′UTR of Top1 mRNA. Since miR-92a-3p's amount positively correlates with CSR efficiency (*SI Appendix*, Fig. S13*D*), it was supposed that miR-92a-3p binds to Top1 3′UTR and suppresses Top1 protein synthesis. To examine its function, miR-92a-3p was knocked down using S-TuD oligos (Fig. 6).

Through the knockdown of miR-92a-3p, CSR has reduced to almost half of the control in wild-type W215 cells; however, this knockdown did not impact CSR in the 3′UTRKO cells, A102, B43, and C1 cells (Fig. 6*A*). The other candidate, miR-499 does not have any effect on CSR. The combination of knockdown of miR-92a-3p and miR-499 does not show any additive effect compared to miR92a-3p (Fig. 6*B*). By implementing this knockdown, the miR-92a-3p amount, normalized by snoRNA202, was lowered to almost 10% of the control in both CIT-stimulated and nonstimulated wild-type W215 cells (Fig. 6*C*). Top1 mRNA normalized by β2M mRNA was not largely changed following the knockdown of miR-92a-3p in wild-type cells (Fig. 6*D*). Germline transcripts of 5′Sμ and 3′Sα regions also did not decrease following this knockdown (Fig. 6 *E* and *F*). Knockdown of miR-92a-3p decreased the frequency of SHM in 5′Sμ core region in W215 cells but not in Top1 3′UTRKO C1 cells (Fig. 6*G* and *SI Appendix*, Table S3). Analysis of AID-dependent DNA break levels using DNA break assay with biotin-dUTP labeling showed a decrease in the DNA break frequency following the knockdown of miR-92a-3p in wild-type cells (Fig. 6*H* and *SI Appendix*, Fig. S15 *A* and *B*). The samples processed without 3′PTP activity show only insufficient difference between the control and knockdown of miR92a-3p, suggesting the presence of 3′phoshate at the break ends produced by Top1-mediated DNA cleavage (*SI Appendix*, Figs. S1 and S15*A*).

Top1 protein amount change by AID activation was compared between the miR-92a-3p-knockdown and control cells. The wild-type W215 cells transfected by the control oligos showed the AID-dependent decrease to Top1 protein (Top1/Actin, 0.8 vs. 1.8, stimulated vs. nonstimulated, Fig. 6 *I*, *Top*). However, this decrease is absent in W215 cells transfected by anti-miR-92a-3p (Top1/Actin, 0.7 vs. 0.8, stimulated vs. not stimulated). In Top1 3′UTRKO-C1 cells, Top1/Actin was unchanged following the knockdown of this miRNA (Fig. 6 *I*, *Bottom*). miR-92a-3p knockdown did not decrease AID protein in both W215 and 3′UTRKO-C1 cells.

Collectively, the knockdown of miR-92a-3p in wild-type cells reproduces the phenotype observed in Top1 3′UTRKO cells, indicating that miR-92a-3p supports the function of Ago2 by binding to Top1 3′UTR and decreasing Top1 protein amount in an AID-dependent manner.

Discussion

In this study, we identified the Top1 3′UTR-mediated contribution of Ago2 and miR-92a-3p in the AID-dependent repression of Top1 protein synthesis.

miR-92a-3p was found in the miRNA cluster, mir-17-92 polycistron, which was amplified in human B cell lymphoma and originally referred to OncomiR-1 (50). This miRNA cluster is well-conserved (51) and they exhibit a variety of expression profiles and functions in the aspects of oncogenesis and development (52, 53). Here, miR-92a-3p is identified as the positive regulator in Ig gene diversification. Our results proposed the base-pairing frame in miR-92a-3p binding to the adjacent region of 5′dAB in Top1 mRNA (*SI Appendix*, Fig. S13*C*), whereas this frame does not follow the classical seed pairing in which guide (g) nucleotides g2-g7 in miRNA align to the target mRNA (54, 55), as g7-g12 nucleotides of miR-92a-3p pair to the adjacent part of 5′dAB in 3′UTR of Top1 mRNA in this case. However, this pairing of miR-92a-3p to 5′dAB via g7-g12 may be possible, because the novel "seed-independent" class of miRNAs was identified and reported from the two independent groups. They both used the method of Ago2-crosslinking immuno-precipitation with RNA ligase that allows the ligation of the miRNAs to the target mRNAs. The miRNA-binding profiles were categorized based on their base-pairing patterns (48, 49). They detected the diversified patterns of paring interactions, in that the central to 3′ side of miRNA sequences base-pair to the targets. In particular, miR-92a showed the highest enrichment in the "nonseed" class (class IV) in one report (48) and "seed pairing plus supplementary 3′ pairing cluster" (k = 2) in the other report (49).

The molecular mechanism of AID's direct action to Ago2 and miR-92a-3p for repressing Top1 protein synthesis still remains elusive. Since AID is presumably an RNA-editing enzyme (35, 56), it would be possible that AID's editing of pri- or pre-miRNA, or the mature sequence of miR-92a-3p converts this miRNA to be more efficient in binding with 5′dAB, which locates in Top1 3′UTR. Although it is purely speculative, g19 cytosine editing to uracil by AID in the 3′ part of matured miR-92a-3p may increase the pairing length and may further stabilize this interaction (*SI Appendix*, Fig. S16). If Ago2-binding AID recognizes the g19 cytosine in miR-92a-3p loaded on Ago2 and edits this cytosine, miR-Top1 mRNA binding may be more stable. This notion is supported by structural analysis of the model of the Ago2 complex and a miRNA, suggesting that the supplementary pairing of the 3′ part of miRNA allows an increase in affinity (55). Congruent with this report, the RNA ligase-mediated analyses of the mRNA-miRNA interaction revealed that the large part of miRNAs exhibit 3′ sequences that bind to their targets and to the seed sequences, suggesting an auxiliary function of 3′ sequences (48, 49).

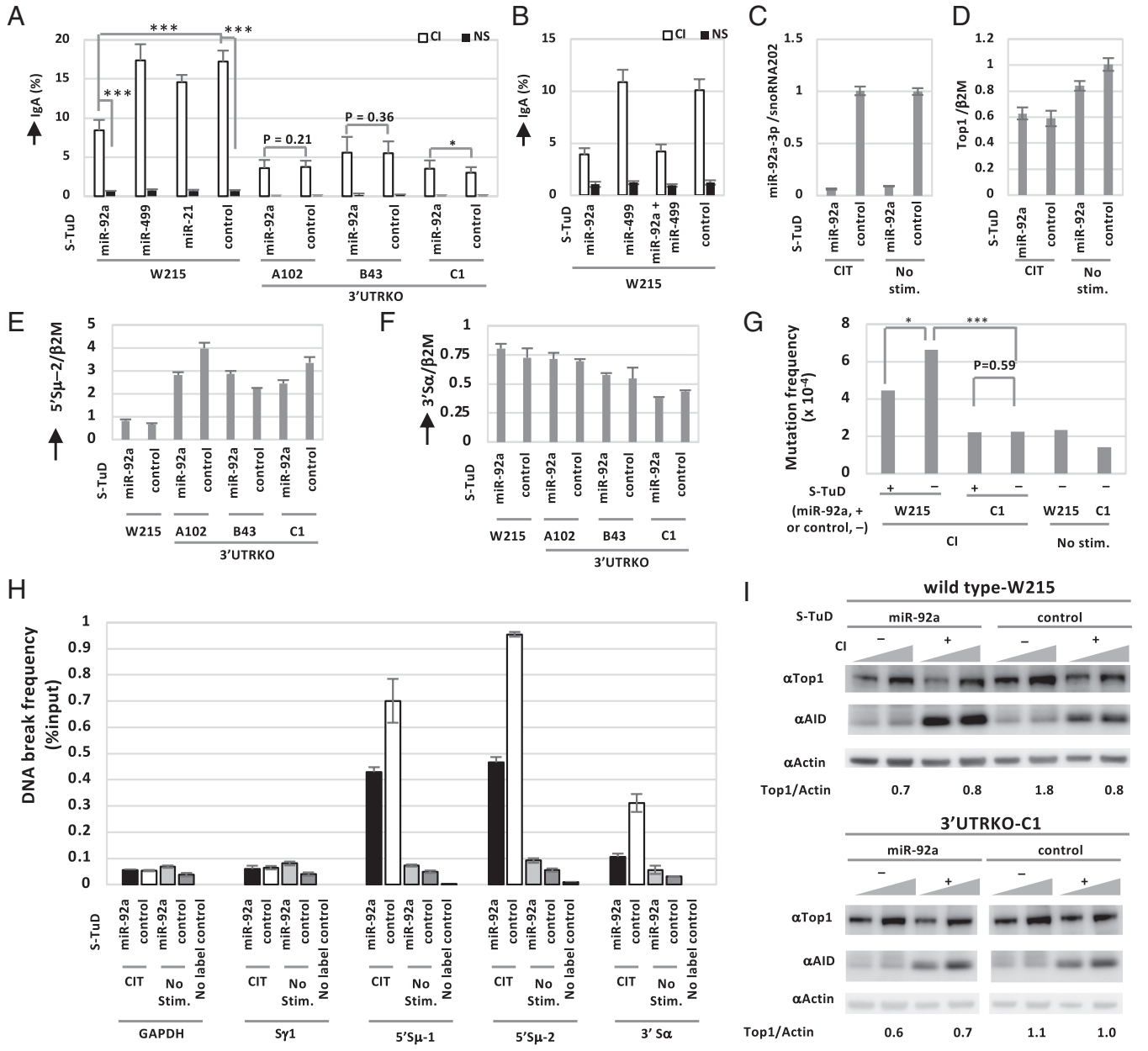

Fig. 6. miR-92a contributes to AID-dependent DNA cleavage and Top1 protein reduction through 3′UTR of Top1 mRNA. (*A*) Effect of miR-92a-3p (miR-92a) knockdown by S-TuD miRNA inhibitors on CSR of CH12 cells, wild-type, and 3′UTRKO-C1 cells. The mean ±SD of three experiments is shown. Statistical significance was calculated using Student's *t* test. Effects of knockdown of miR-499-5p (miR-499) and miR-21-5p (miR-21) are also shown. (*B*) IgA switching efficiencies after transfection with S-TuD miRNA inhibitors against miR-92a and miR-499, respectively, or in combination. (*C*) The amount of miR-92a-3p normalized by snoRNA202 in miR-92a-3p knockdown. The mean ±SD of triplicate of the qPCR experiment is shown. (*D*–*F*) Expression of Top1 (*D*), Sμ (*E*)- and Sα (*F*)-germline transcripts following the knockdown of miR-92a-3p. The mean ±SD of the three experiments is shown. (*G*) Somatic hypermutation frequency in wild-type and 3′UTRKO-C1 cells after the knockdown of miR-92a-3p. Statistical significance was calculated using a Fisher's exact test. *$P < 0.05$; ***$P < 0.001$. + means miR-92a-3p and— means the control S-TuD oligos. (*H*) AID-dependent DNA break frequency in the cells of knockdown of miR-92a-3p in wild-type cells detected by biotin-16-dUTP labeling. CIT-stimulated and nonstimulated cells were compared. The primers are described in Dataset S5. (*I*) Top1 protein amount in PBS-TritonX-100 fraction in wild-type and Top1 3′UTRKO-C1 cells following the knockdown of miR-92a-3p and revealed by a western blot. The intensity of each band was quantified using ImageJ to calculate the Top1/actin ratio. The representative picture of the three experiments is shown. The triangles show the loading amount of the lysates, the right lane contains 1.5 volume of the left lane in each sample.

On the other hand, Top1 mRNA editing by AID was not strongly anticipated, because no remarkable C to U editing was identified in Top1 mRNA in our PAR-CLIP experiments (Datasets S1 and S2) with anti-Ago2 antibody, suggesting that Top1 mRNA is not the direct RNA editing target of AID.

Top1 protein synthesis was decreased in an AID-dependent and Top1 3′UTR-mediated manner. Polysome fractionation suggested that not by translational block but by elimination of Top1 mRNA by AID through Top1 3′UTR. This suggests the possibility of function of miRNA-Ago2-AID pathway to Top1 mRNA in sucrose gradient. However, it is still questionable whether miRNA-Ago2-complex can be active to eliminate their target mRNA in polysome fractionation. As the cell lysis buffer and the sucrose solution used in this polysome analysis consisted by HEPES-KOH, KCl, MgCl2 and 0.05% NP-40 and supplemented by the several inhibitors to RNases, proteinases and translation, these solutions may not completely inhibit the activity of miRNA-Ago2 complex. Interestingly, approximately 60% of Top2a mRNA, a target of miR-139-5a (57), was lost during fractionation.

Although questions remain about the molecular mechanisms underlying the AID-dependent and 3′UTR-mediated reduction of Top1 mRNA, the newly synthesized Top1 proteins are also decreased in the same fashion. Together with the other pieces of evidence, such as 1) 3′UTR requirement in AID-dependent DNA cleavage and Ago2 binding to Top1 mRNA, 2) interaction of AID and Ago2, 3) miR-92a-3p's positive effect on Top1 protein decrease and DNA cleavage through Top1 3′UTR, leads to a speculative answer, that binding of the AID-Ago2-miR92a-3p tertiary complex to Top1 3′UTR causes a posttranscriptional decrease in Top1 mRNA. Ultimately this AID-dependent, 3′UTR-mediated Top1 decrease alters the DNA secondary structure to non-B-DNA at IgH S regions, facilitating AID-dependent DNA cleavage (Fig. 7) (15, 16).

In our experiments, total Top1 mRNA did not directly correlate with soluble Top1 protein amount (Fig. 3*C* and *SI Appendix*, Fig. S8). The reason is unknown; however, complexity of subcellular localization of Top1 mRNA will be one of them. For example, we have detected localization of Top1 mRNA in P-bodies which is the condensation of repressed mRNA regulons (58) (*SI Appendix*, Fig. S17). If the Top1 mRNA is sequestrated to these ill-defined cytoplasmic RNA bodies and further regulated, Top1 mRNA amount in whole-cell extract could not be reliable to fully explain the change of soluble Top1 protein according to the AID activation.

T4PNK with 3'PTP activity has not previously been applied in DNA break assay using Bio-dUTP and TdT, however, we have found that addition of 3'PTP treatment increases the sensitivity of DNA break assay (Fig. 2*F* and *SI Appendix*, Fig. S15*A*). 3′phosphates at the DNA break ends are generally formed by irradiation, alkylating reagents, oxidation, DNase2, Top2 or Top1 (44, 59, 60). Top1-mediated DNA break ends are supposed to be repaired by Top1 protein degradation by the proteasome, followed by processing with TDP1 to remove catalytic tyrosine in the remnant of Top1, which leaves 3′phosphates at the DNA break ends (61) (*SI Appendix*, Fig. S1). Even without 3′PTP, we could still detect the difference between stimulated and non-stimulated, but it was not sensitive enough to detect the difference between wild-type and 3′UTRKO cells. This suggests that some of the 3′phosphates will be removed in vivo by the endogenous 3′phosphatases such as PNKP, aprataxin, and/or apurinic/apyrimidinic endonuclease 1 in the cells (11). Considering the other possibilities, irradiation and oxidation can be excluded as the cause of AID-dependent DNA cleavage. DNase2 generally localizes in lysozyme to eliminate the exogenous DNA or in nucleus to degrade DNA at the occasion of apoptosis (62). As we removed dead cells from the cells used for this DNA break assay, the involvement of DNase2 is unlikely. Because AID-dependent breaks are staggered type DNA break ends but not the blunt type double-stranded DNA break (63), Top2 is not considered as the responsible enzyme in this case. Since base excision repair-induced single-stranded breaks (SSBs) by APE1 form 5′-terminal abasic sugar and 3′-OH, and Top1-induced SSBs leaves 3′phosphate after removal of tyrosine residue by TDP1 (44, 60), presence of 3′-phosphate at AID-dependent DNA break ends suggests the contribution of Top1 (*SI Appendix*, Fig. S1). Therefore we again propose that Top1 cleaves IgH gene in an AID-dependent manner (Fig. 7). However, a concern will remain that whether the reduced half amount of Top1 can really cut the non-B-DNA in IgH gene. It should be addressed in the future.

In summary, we here show AID-dependent control of Top1 protein synthesis through miR-92a-3p and Ago2; however, further research will be required for identifying the AID's precise molecular function, which uncovers interaction mechanisms between this miRNA and Top1 mRNA and RNA-editing by AID. Moreover, it is supposed that AID has another function to provoke DNA cleavage (Fig. 7). We previously found that 24 to 48-h Top1 knockdown alone (without AID activation) induces non-B-DNA structure; however, it does not provoke sufficient level of DNA break or CSR increment (15). In short, a Top1 decrease is necessary for efficient DNA cleavage but not enough to trigger DNA cleavage within a few days. Compared to that, induction of genomic instability is possible if Top1 knockdown is persistent (23, 24). This indicates that another type of DNA damage will trigger DNA cleavage in chronic Top1 decrease. Features of AID other than Top1 reduction could also be the focus of further studies.

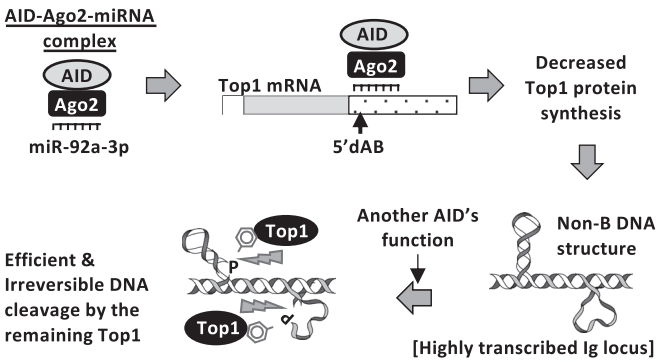

Fig. 7. Possible regulation of AID-dependent decrease in Top1 protein synthesis and enhancement of DNA cleavage by the Ago2-miR complex. AID promotes loading of the Ago2-miR-92a-3p complex onto the 5′dAB sites in 3′UTR of Top1 mRNA, which decreases Top1 protein synthesis. As the result, the non-B-DNA structures accumulate at this actively transcribed IgH gene locus, enabling efficient DNA cleavage. Since Top1 decrease is necessary but not sufficient for provoking DNA breaks, AID's function separate from Top1 reduction triggers highly frequent and irreversible DNA cleavage mediated by the remaining Top1.

Materials and Methods

Cell Culture and Stimulation to Induce AID Expression. CH12 cells were cultured as described in previous work (15). AID was induced using a combination of cytokines CD40 ligand (generated in our laboratory), IL-4 (Wako), and TGF-β (R&D). AID-ER was activated using 1 μM of 4-OHT.

Additional details of the other methods used in this study are reported in *SI Appendix*.

Data, Materials, and Software Availability. BioSample accession number of the raw data obtained by next-generation sequencing (NGS) is PRJNA887827 (64). The processed data by NGS are available in Datasets S1–S3. Other data of the additional protocols are available in the main manuscript and *SI Appendix* with Dataset S5. Cell lines and plasmids are available from the corresponding author upon request.

ACKNOWLEDGMENTS. This research was supported by Japan Society for the Promotion of Science KAKENHI, JP22H00449 to T.H. and Grant Number JP22K06202 to M.K. We thank to the past and present lab members of Immunology and Genomic Medicine, Center for Cancer Immunotherapy and Immunobiology, and Center for Genomic Medicine, Graduate School of Medicine, Kyoto University for sharing reagents and for engaging in helpful discussions. In particular, we extend our thanks to Ms. Yoko Kitawaki and Ms. Maki Sasanuma for the technical assistance and to Dr. Norimichi Nomura (Department of Cell Biology, Graduate School of Medicine, Kyoto University) for the purification of anti-AID antibody, #488-5.

Author affiliations: [a]Immunology and Genomic Medicine, Center for Cancer Immunotherapy and Immunobiology, Graduate School of Medicine, Kyoto University, Kyoto 606-8501, Japan; and [b]Center for Genomic Medicine, Graduate School of Medicine, Kyoto University, Kyoto 606-8501, Japan

Author contributions: M.K. and T.H. designed research; M.K. and M.S. performed research; M.K., H.W., K.H., and F.M. contributed new reagents/analytic tools; M.K., H.W., K.H., F.M., and T.H. analyzed data; and M.K., K.H., F.M., and T.H. wrote the paper.

Reviewers: N.K., University of Texas Health Science Center at Houston; and D.K., Tokyo Rika Daigaku–Noda Campus.

1. M. Muramatsu *et al.*, Class switch recombination and hypermutation require activation-induced cytidine deaminase (AID), a potential RNA editing enzyme. *Cell* **102**, 553–563 (2000).
2. P. Revy *et al.*, Activation-induced cytidine deaminase (AID) deficiency causes the autosomal recessive form of the Hyper-IgM syndrome (HIGM2). *Cell* **102**, 565–575 (2000).
3. H. Arakawa, J. Hauschild, J.-M. Buerstedde, Requirement of the activation-induced deaminase (AID) gene for immunoglobulin gene conversion. *Science* **295**, 1301–1306 (2002).
4. N. A. Begum, H. Nagaoka, M. Kobayashi, T. Honjo, "Molecular Mechanisms of AID Function" in *Molecular Biology of B Cells*, F. W. Alt, T. Honjo, A. Radbruch, M. Reth, Eds. (Elsevier Ltd, 2014), pp. 305–344.
5. J. B. Leppard, J. J. Champoux, Human DNA topoisomerase I: Relaxation, roles, and damage control. *Chromosoma* **114**, 75–85 (2005).
6. K. C. Nitiss, J. L. Nitiss, L. A. Hanakahi, DNA damage by an essential enzyme: A delicate balance act on the tightrope. *DNA Repair* **82**, 102639 (2019).
7. Y. Pommier, Topoisomerase I inhibitors: Camptothecins and beyond. *Nat. Rev. Cancer* **6**, 789–802 (2006).
8. S. Katyal *et al.*, Aberrant topoisomerase-1 DNA lesions are pathogenic in neurodegenerative genome instability syndromes. *Nat. Neurosci.* **17**, 813–821 (2014).
9. S. Katyal *et al.*, TDP1 facilitates chromosomal single-strand break repair in neurons and is neuroprotective in vivo. *EMBO J.* **26**, 4720–4731 (2007).
10. L. C. Dumitrache, P. J. McKinnon, Polynucleotide kinase-phosphatase (PNKP) mutations and neurologic disease. *Mech. Ageing Dev.* **161**, 121–129 (2017).
11. T. Takahashi *et al.*, Aprataxin, causative gene product for EAOH/AOA1, repairs DNA single-strand breaks with damaged 3′-phosphate and 3′-phosphoglycolate ends. *Nucleic Acids Res.* **35**, 3797–3809 (2007).
12. A. Bacolla, M. Wojciechowska, B. Kosmider, J. E. Larson, R. D. Wells, The involvement of non-B DNA structures in gross chromosomal rearrangements. *DNA Repair* **5**, 1161–1170 (2006).
13. A. Bacolla, R. D. Wells, Non-B DNA conformations, genomic rearrangements, and human disease. *J. Biol. Chem.* **279**, 47411–47414 (2004).
14. R. D. Wells, Non-B DNA conformations, mutagenesis and disease. *Trends Biochem. Sci.* **32**, 271–278 (2007).
15. M. Kobayashi *et al.*, AID-induced decrease in topoisomerase 1 induces DNA structural alteration and DNA cleavage for class switch recombination. *Proc. Natl. Acad. Sci. U.S.A.* **106**, 22375–22380 (2009).
16. M. Kobayashi *et al.*, Decrease in topoisomerase I is responsible for activation-induced cytidine deaminase (AID)-dependent somatic hypermutation. *Proc. Natl. Acad. Sci. U.S.A.* **108**, 19305–19310 (2011).
17. B.-G. Ju *et al.*, A topoisomerase IIb–mediated dsDNA break required for regulated transcription. *Science* **312**, 1798–1802 (2006).
18. T. Doi *et al.*, The C-terminal region of activation-induced cytidine deaminase is responsible for a recombination function other than DNA cleavage in class switch recombination. *Proc. Natl. Acad. Sci. U.S.A.* **106**, 2758–2763 (2009).
19. M. J. Lippert *et al.*, Role for topoisomerase 1 in transcription-associated mutagenesis in yeast. *Proc. Natl. Acad. Sci. U.S.A.* **108**, 698–703 (2011).
20. T. Takahashi, G. Burguiere-Slezak, P. A. Van der Kemp, S. Boiteux, Topoisomerase 1 provokes the formation of short deletions in repeated sequences upon high transcription in Saccharomyces cerevisiae. *Proc. Natl. Acad. Sci. U.S.A.* **108**, 692–697 (2011).
21. N. Kim *et al.*, Mutagenic processing of ribonucleotides in DNA by yeast topoisomerase 1. *Science* **332**, 1561–1564 (2011).
22. L. Hubert Jr., Y. Lin, V. Dion, J. H. Wilson, Topoisomerase 1 and single-strand break repair modulate transcription-induced CAG repeat contraction in human cells. *Mol. Cell. Biol.* **31**, 3105–3112 (2011).
23. Z. H. Miao *et al.*, Nonclassic functions of human topoisomerase I: Genome-wide and pharmacologic analyses. *Cancer Res.* **67**, 8752–8761 (2007).
24. R. Nakatani, M. Nakamori, H. Fujimura, H. Mochizuki, M. P. Takahashi, Large expansion of CTG·CAG repeats is exacerbated by MutSβ in human cells. *Sci. Rep.* **5**, 1–11 (2015).
25. A. Husain *et al.*, Chromatin remodeller SMARCA4 recruits topoisomerase 1 and suppresses transcription-associated genomic instability. *Nat. Commun.* **7**, 10549 (2016).
26. C.-P. Lin, Y. Ban, Y. L. Lyu, S. D. Desai, L. F. Liu, A ubiquitin-proteasome pathway for the repair of topoisomerase I-DNA covalent complexes. *J. Biol. Chem.* **283**, 21074–21083 (2008).
27. J. Xu, A. Husain, W. Hu, T. Honjo, M. Kobayashi, Ape1 is dispensable for s-region cleavage but required for its repair in class switch recombination. *Proc. Natl. Acad. Sci. U.S.A.* **111**, 17242–17247 (2014).
28. L. F. R. Gebert, I. J. MacRae, Regulation of microRNA function in animals. *Nat. Rev. Mol. Cell Biol.* **20**, 21–37 (2018).
29. G. Hutvagner, M. J. Simard, Argonaute proteins: Key players in RNA silencing. *Nat. Rev. Mol. Cell Biol.* **9**, 22–32 (2008).
30. M. Ha, V. N. Kim, Regulation of microRNA biogenesis. *Nat. Rev. Mol. Cell Biol.* **15**, 509–524 (2014).
31. E. Huntzinger, E. Izaurralde, Gene silencing by microRNAs: Contributions of translational repression and mRNA decay. *Nat. Rev. Genet.* **12**, 99–110 (2011).
32. W. Yang *et al.*, Modulation of microRNA processing and expression through RNA editing by ADAR deaminases. *Nat. Struct. Mol. Biol.* **13**, 13–21 (2006).
33. Y. Kawahara, B. Zinshteyn, T. P. Chendrimada, R. Shiekhattar, K. Nishikura, RNA editing of the microRNA-151 precursor blocks cleavage by the Dicer-TRBP complex. *EMBO Rep.* **8**, 763–769 (2007).
34. T. Nonaka *et al.*, Carboxy-terminal domain of AID required for its mRNA complex formation in vivo. *Proc. Natl. Acad. Sci. U.S.A.* **106**, 2747–2751 (2009).
35. G. Liang *et al.*, RNA editing of hepatitis B virus transcripts by activation-induced cytidine deaminase. *Proc. Natl. Acad. Sci. U.S.A.* **110**, 2246–2251 (2013).
36. S. Zheng *et al.*, Non-coding RNA generated following lariat debranching mediates targeting of AID to DNA. *Cell* **161**, 762–773 (2015).
37. L. A. Gilbert *et al.*, CRISPR-mediated modular RNA-guided regulation of transcription in eukaryotes. *Cell* **154**, 442–451 (2013).
38. S. Cheloufi, C. O. Dos Santos, M. M. W. Chong, G. J. Hannon, A dicer-independent miRNA biogenesis pathway that requires Ago catalysis. *Nature* **465**, 584–589 (2010).
39. E. Herrera-Carrillo, B. Berkhout, Dicer-independent processing of small RNA duplexes: Mechanistic insights and applications. *Nucleic Acids Res.* **45**, 10369–10379 (2017).
40. M. Hafner *et al.*, Transcriptome-wide identification of RNA-binding protein and MicroRNA target sites by PAR-CLIP. *Cell* **141**, 129–141 (2010).
41. T. Doi, K. Kinoshita, M. Ikegawa, M. Muramatsu, T. Honjo, De novo protein synthesis is required for the activation-induced cytidine deaminase function in class-switch recombination. *Proc. Natl. Acad. Sci. U.S.A.* **100**, 2634–2638 (2003).
42. J. M. Beekman, G. F. Allan, S. Y. Tsai, M. J. Tsai, B. W. O'Malley, Transcriptional activation by the estrogen receptor requires a conformational change in the ligand binding domain. *Mol. Endocrinol.* **7**, 1266–1274 (1993).
43. D. Picard, Steroid-binding domains for regulating the functions of heterologous proteins in cis. *Trends Cell Biol.* **3**, 278–280 (1993).
44. K. W. Caldecott, DNA single-strand break repair and human genetic disease. *Trends Cell Biol.* **32**, 733–745 (2022).
45. V. Gandin *et al.*, Polysome fractionation and analysis of mammalian translatomes on a genome-wide scale. *J. Vis. Exp.*, 10.3791/51455 (2014).
46. L. Stalder *et al.*, The rough endoplasmatic reticulum is a central nucleation site of siRNA-mediated RNA silencing. *EMBO J.* **32**, 1115–1127 (2013).
47. R. Aviner *et al.*, Proteomic analysis of polyribosomes identifies splicing factors as potential regulators of translation during mitosis. *Nucleic Acids Res.* **45**, 5945–5957 (2017).
48. A. Helwak, G. Kudla, T. Dudnakova, D. Tollervey, Mapping the human miRNA interactome by CLASH reveals frequent noncanonical binding. *Cell* **153**, 654–665 (2013).
49. M. J. Moore *et al.*, miRNA–target chimeras reveal miRNA 3′-end pairing as a major determinant of Argonaute target specificity. *Nat. Commun.* **6**, 1–17 (2015).
50. L. He *et al.*, A microRNA polycistron as a potential human oncogene. *Nature* **435**, 828–833 (2005).
51. C. P. Concepcion, C. Bonetti, A. Ventura, The microRNA-17-92 family of microRNA clusters in development and disease. *Cancer J.* **18**, 262–267 (2012).
52. J. T. Mendell, miRiad roles for the miR-17-92 cluster in development and disease. *Cell* **133**, 217–222 (2008).
53. E. Mogilyansky, I. Rigoutsos, The miR-17/92 cluster: A comprehensive update on its genomics, genetics, functions and increasingly important and numerous roles in health and disease. *Cell Death Differ.* **20**, 1603–1614 (2013).
54. B. P. Lewis, C. B. Burge, D. P. Bartel, Conserved seed pairing, often flanked by adenosines, indicates that thousands of human genes are microRNA targets. *Cell* **120**, 15–20 (2005).
55. J. Sheu-Gruttadauria, Y. Xiao, L. F. Gebert, I. J. MacRae, Beyond the seed: Structural basis for supplementary microRNA targeting by human Argonaute2. *EMBO J.* **38**, e101153 (2019).
56. T. Honjo, K. Kinoshita, M. Muramatsu, Molecular mechanism of class switch recombination: Linkage with somatic hypermutation. *Annu. Rev. Immunol.* **20**, 165–196 (2002).
57. M. Pajic *et al.*, miR-139-5p modulates radiotherapy resistance in breast cancer by repressing multiple gene networks of DNA repair and ROS defense. *Cancer Res.* **78**, 501–515 (2018).
58. A. Hubstenberger *et al.*, P-body purification reveals the condensation of repressed mRNA regulons. *Mol. Cell* **68**, 144–157.e5 (2017).
59. F. Karimi-Busheri, J. Lee, A. E. Tomkinson, M. Weinfeld, Repair of DNA strand gaps and nicks containing 3′-phosphate and 5′-hydroxyl termini by purified mammalian enzymes. *Nucleic Acids Res.* **26**, 4395–4400 (1998).
60. S. Boiteux, M. Guillet, Abasic sites in DNA: Repair and biological consequences in Saccharomyces cerevisiae. *DNA Repair* **3**, 1–12 (2004).
61. Y. Pommier *et al.*, Repair of and checkpoint response to topoisomerase I-mediated DNA damage. *Mutat. Res.* **532**, 173–203 (2003).
62. C. J. Evans, R. J. Aguilera, DNase II: Genes, enzymes and function. *Gene* **322**, 1–15 (2003).
63. X. Chen, K. Kinoshita, T. Honjo, Variable deletion and duplication at recombination junction ends: Implication for staggered double-strand cleavage in class-switch recombination. *Proc. Natl. Acad. Sci. U.S.A.* **98**, 13860–13865 (2001).
64. M. Kobayashi *et al.*, *RNA* sequencing enriched to Ago2. *NCBI Bioproject*. https://www.ncbi.nlm.nih.gov/bioproject/PRJNA887827. Accessed 7 October 2022.